doi:10.1093/brain/awu354 BRAIN 2015: 138; 440–455 | 440

BRAIN
A JOURNAL OF NEUROLOGY

Genetic manipulation of adult-born hippocampal neurons rescues memory in a mouse model of Alzheimer's disease

Kevin Richetin,[1,2] Clémence Leclerc,[1,2,3] Nicolas Toni,[4] Thierry Gallopin,[3] Stéphane Pech,[1,2] Laurent Roybon[5] and Claire Rampon[1,2]

In adult mammals, neural progenitors located in the dentate gyrus retain their ability to generate neurons and glia throughout lifetime. In rodents, increased production of new granule neurons is associated with improved memory capacities, while decreased hippocampal neurogenesis results in impaired memory performance in several memory tasks. In mouse models of Alzheimer's disease, neurogenesis is impaired and the granule neurons that are generated fail to integrate existing networks. Thus, enhancing neurogenesis should improve functional plasticity in the hippocampus and restore cognitive deficits in these mice. Here, we performed a screen of transcription factors that could potentially enhance adult hippocampal neurogenesis. We identified *Neurod1* as a robust neuronal determinant with the capability to direct hippocampal progenitors towards an exclusive granule neuron fate. Importantly, *Neurod1* also accelerated neuronal maturation and functional integration of new neurons during the period of their maturation when they contribute to memory processes. When tested in an APPxPS1 mouse model of Alzheimer's disease, directed expression of *Neurod1* in cycling hippocampal progenitors conspicuously reduced dendritic spine density deficits on new hippocampal neurons, to the same level as that observed in healthy age-matched control animals. Remarkably, this population of highly connected new neurons was sufficient to restore spatial memory in these diseased mice. Collectively our findings demonstrate that endogenous neural stem cells of the diseased brain can be manipulated to become new neurons that could allow cognitive improvement.

1 Université de Toulouse, UPS, Centre de Recherches sur la Cognition Animale, 118 route de Narbonne, F-31062 Toulouse Cedex 4, France
2 CNRS, Centre de Recherches sur la Cognition Animale, F-31062 Toulouse, France
3 Laboratoire de Neurobiologie, ESPCI ParisTech, UMR 7637, Paris, France
4 Department of Fundamental Neurosciences, University of Lausanne, Rue du Bugnon 9, CH-1005 Lausanne, Switzerland
5 Stem Cell Laboratory for CNS Disease Modeling, Department of Experimental Medical Science, Wallenberg Neuroscience Centre, Lund University, BMC A10, 221 84 Lund, Sweden

Correspondence to: Claire Rampon,
CNRS UMR 5169, Centre de Recherches sur la Cognition Animale (CRCA),
Université Paul Sabatier, 118 route de Narbonne,
31062 Toulouse Cedex 4, France
E-mail: claire.rampon@univ-tlse3.fr

Keywords: adult neurogenesis; memory; Alzheimer's disease; *Neurod1*; hippocampus

Abbreviations: bHLH = basic helix-loop-helix; dpi = days post-injection; NeuN = neuronal nuclei

Received June 11, 2014. Revised October 14, 2014. Accepted October 15, 2014. Advance Access publication December 17, 2014

Introduction

In the mammalian brain, new neurons are produced in the hippocampus throughout adult life (Altman and Das, 1965; Eriksson *et al.*, 1998). These neurons become structurally and functionally integrated into the hippocampal circuitry where they critically contribute to hippocampal-dependent learning and memory processes (Kee *et al.*, 2007; Aimone *et al.*, 2011; Gu *et al.*, 2012). Compelling evidence demonstrates that in several memory tasks, the inhibition of adult hippocampal neurogenesis leads to memory impairments (Shors *et al.*, 2001; Goodman *et al.*, 2010) while the enhancement of neurogenesis improves memory performances (Kempermann *et al.*, 1998; van Praag *et al.*, 1999). Alzheimer's disease is one of the most common causes of dementia and cognitive impairments in the elderly. Initial quantification of proliferative and neurogenic markers in post-mortem tissue of patients with Alzheimer's disease has led to rather contradictory results and interpretations (Jin *et al.*, 2004; Boekhoorn *et al.*, 2006; Li *et al.*, 2008; Zhang *et al.*, 2008). A better understanding was recently provided by reports showing that adult hippocampal neurogenesis is differentially affected during the progression of the disease in patients (Perry *et al.*, 2012; Ekonomou *et al.*, 2014; Gomez-Nicola *et al.*, 2014). Although compensatory increased cell proliferation was observed at early stages of the disease, it remains to be determined to which extent this might relate to glial or vascular processes (Song *et al.*, 2002; Boekhoorn *et al.*, 2006; Verwer *et al.*, 2007; Ekonomou *et al.*, 2014). Recent data indicate that proliferation in Alzheimer's disease human brains mainly results from microglia and occurs at the vicinity of amyloid plaques (Marlatt *et al.*, 2014). These data are in line with other studies reporting that proliferating cells do not become mature neurons in the Alzheimer's disease brain (Li *et al.*, 2008; Ekonomou *et al.*, 2014).

Interestingly, at the functional level, low proliferation and differentiation capacities of adult hippocampal stem cells correlated with memory dysfunction in human (Coras *et al.*, 2010). In transgenic mouse models of Alzheimer's disease, a large number of data were obtained that diverged depending on the mouse line, mouse genetic background and gender, and disease severity (Marlatt and Lucassen, 2010; Marlatt *et al.*, 2013). However, a general picture has emerged indicating that adult hippocampal neurogenesis is altered in amyloidogenic mouse models of Alzheimer's disease (Verret *et al.*, 2007; Demars *et al.*, 2010; Krezymon *et al.*, 2013). These alterations seem to precede or at least occur early in the development of the pathology in mice (Demars *et al.*, 2010; Krezymon *et al.*, 2013). Altogether these data indicate that enhancing endogenous neurogenesis may be a potential therapeutic target to improve hippocampal function in Alzheimer's disease.

Pharmacological strategies that enhance adult hippocampal neurogenesis in mouse models of Alzheimer's disease, with the aim to restore memory function, have been developed (Fiorentini *et al.*, 2010; Wang *et al.*, 2010). However, nowadays hopes have been raised that cell therapeutic intervention would become available through the manipulation of endogenous stem cells (Marr *et al.*, 2010). The identification of molecular targets regulating the production, maturation and functional integration of new neurons has remained a hindrance to such endeavour. Among them, it was reported that the cell-intrinsic proneural bHLH (basic helix-loop-helix) transcription factor *Neurod1* is required for newborn granule cells to fully mature and survive in the healthy adult brain (Gao *et al.*, 2009). In this study, we manipulated dividing cells and their progeny in the dentate gyrus in order to enhance maturation and functional integration of granule neurons in the adult mouse hippocampus. Using retrovirus-mediated gene delivery in adult neural progenitors of the healthy brain, we performed a bHLH transcription factor screen *in vivo* and identified *Neurod1* as a strong molecule candidate to direct adult hippocampal progenitors towards an exclusive neuronal fate and stimulate their terminal neuronal differentiation. Then, *Neurod1* gene delivery was applied to adult neural progenitors of a mouse model of Alzheimer's disease in an attempt to improve neurogenesis and restore cognitive deficits in these mice.

Materials and methods

Retroviral vectors

Enhanced green fluorescence protein (eGFP), *Neurog2*, *Neurod1* and *Neurod2*-expressing Moloney murine leukemia-derived retroviral vectors (pCMMP-IRES2eGFP-WPRE, pCMMP-Neurod1-IRES2eGFP-WPRE, pCMMP-Neurod2-IRES2eGFP-WPRE and pCMMP-Neurog2-IRES2eGFP-WPRE) were produced and titrated as previously described (Hofstetter *et al.*, 2005; Roybon *et al.*, 2009). The final titre of each retrovirus ranged from 0.5×10^9 to 3×10^9 TU/ml. The integration of these retroviral vectors into the host genome occurs only during cell division and was not affected by the mice genotype (data not shown). Thus, the expression of *GFP*, *Neurog2*, *Neurod1* or *Neurod2* transgenes is restricted to cells dividing shortly after viral injection, allowing visualization and birth dating of transduced cells.

Animals and stereotaxic delivery of the retroviral vectors

Four month-old female C57Bl/6 mice (Charles River Laboratories) and 8–9 month-old (middle age) female APPsw 695/PS1dE9 (Jankowsky *et al.*, 2004) mice were used. Three days before virus injection, mice were placed in individual cages containing a running wheel to enhance cell division and were returned to their home cage with their cage mates after viral injection. Mice were anaesthetized with a mixture of ketamine and xylazine and injected with 0.5 µl (at a rate of 0.1 µl/min) of either viral solution bilaterally into the dentate gyrus according to stereotaxic coordinates (Bregma: antero-

posterior –2 mm, lateral ± 1.6 mm, dorso-ventral −2.5 mm from skull). After recovery in a heated chamber, mice were returned to their home cages. Experiments and analysis were all conducted by experimenters blind to the experimental conditions. All experiments were performed in strict accordance with the recommendations of The European Communities Council Directive (86/609/EEC), The French National Committee (87/848) and the guide for the Care and Use of Laboratory Animals of the National Institutes of Health (NIH publication number 85–23). Approval for this study was obtained from FRBT-01 Ethical Committee. All efforts were made to improve animals' welfare and minimize animals suffering.

Immunohistochemistry

At different time-points after viral injection, mice were deeply anesthetized and transcardially perfused with 4% paraformaldehyde. Series of one in six [or one in three for 28 and 56 days post-injection (dpi)], 50-µm thick coronal sections were incubated in a solution of mouse anti-NeuN (1:1000, Millipore), rabbit anti-GFP (1:500, Torrey Pines), goat anti-GFP (1:500, Torrey Pines) and rabbit anti-GFAP (1:500, Millipore) for 48 h at 4°C. Sections surrounding the injection site and displaying signs of lesion were discarded. After several rinses in phosphate-buffered saline containing 0.25% Triton-X (PBST), sections were incubated for 90 min at room temperature in a solution of: Alexa Fluor® 488-conjugated highly cross-adsorbed donkey anti-goat, Alexa Fluor® 488-conjugated donkey anti-rabbit, Alexa Fluor® 555-conjugated donkey anti-rabbit, Alexa Fluor® 555-conjugated donkey anti-goat or Alexa Fluor® 647-conjugated donkey anti-mouse (all at 1:500; Life Technologies) in PBST. Sections were rinsed intensively and mounted onto slides, coverslipped using Mowiol® mixed with Hoechst (1:10 000; Life Technologies) and stored at 4°C. Sections surrounding the injection site and displaying signs of lesion were discarded.

Gross morphological characterization of GFP-labelled cells

Quantification of GFP-labelled (GFP+) cells was conducted from a 1-in-3 sections spaced at 150 µm using an Olympus BX-51 microscope equipped with Mercator software (Explora Nova). Slides were coded before analysis; the experimenter was blind to genotype until all samples were counted. Based on their morphological parameters, all GFP+ cells by hippocampal section were classified as glial or neuron cells at 14 and 21 dpi. Glial cells show a large spheroid or pyramidal soma with ramified processes. In our study, we focused on GFP+ neurons displayed an apical dendritic tree extending through the granular cell layer and reaching the molecular layer.

Quantification and determination of cell phenotype

Quantification of GFP-labelled (GFP+) cells per brain was conducted from a 1-in-3 sections spaced at 150 µm using an Olympus BX-51 microscope equipped with Mercator software (Explora Nova). The total number of GFP+ cells was estimated by the sum of GFP+ cells found in 1-in-3 sections multiplied by three. Cell phenotype was determined from 25 GFP+ cells per mouse analysed for co-localization with either NeuN or GFAP at 0.5-µm step intervals over their entire *z*-axis using a ×63 oil-immersion objective of a confocal laser-scanning microscope (TCS SP5; Leica). Labelled cells were rotated in orthogonal planes (*x* and *y*) to verify double labelling. All analyses were done in sequential scanning mode to prevent crossover between channels. The estimated fraction of GFP+ cells co-labelled with NeuN or GFAP was calculated for each animal. Absolute numbers of GFP+/NeuN+, GFP+/GFAP+ and GFP+/NeuN−/GFAP− were obtained by multiplying the corresponding estimated fraction of co-labelled GFP+ cells by the total number of GFP+ cells for each animal.

Axonal growth analysis of GFP+ cells

The overall axonal growth of GFP+ neurons was measured by imaging brain sections containing the hippocampus and stained for GFP and counterstained with Hoechst. The growth of axonal fibres was measured with Mercator software (Explora Nova) as previously described (Krezymon *et al.*, 2013). Briefly, a straight line connecting the ends of the two blades of the dentate gyrus was drawn and served as a starting point to trace a line following GFP+ axonal fibres, along the border between the stratum pyramidale and stratum radiatum. A total of 10–12 sections per mouse were used for each time point.

Three-dimensional analyses of GFP+ neurons

At 14 dpi, 10–15 GFP+ neurons per mouse were analysed by acquisition of z-series of 50–75 optical sections at 0.5-µm intervals, with a ×40 oil lens, digital zoom of 1.7, with a TCS SP5 (Leica Microsystem) confocal system. To image only the GFP+ neurons that were fully contained in the section, labelled neurons with processes that impinged upon the 3-µm wide zones located at the top and bottom of the section were excluded from the study. Three-dimensional reconstructions of series of confocal images were conducted using Imaris XT (Bitplane AG) on deconvolved images (Huygens SVI). Total dendritic length and number of dendritic branching were automatically calculated from 3D reconstructions.

Dendritic spine density and spine shape analysis

Dendritic processes of GFP+ neurons in the middle molecular layer were analysed by acquiring *z*-series of 30–50 optical sections at 0.13-µm intervals, with a ×63 oil lens, digital zoom of 5, with a TCS SP5 (Leica Microsystem) confocal system. Before analysis, files were subjected to seven iterations of deconvolution with the Huygens Essential deconvolution software (SVI). Confocal images were imported into Imaris XT (Bitplane AG) and for analysis. Drift correction, particle tracking, and surface tracking were done using autoregressive tracking algorithms. Dendritic spines were defined as protrusions from the dendritic shaft and classified based on their shape according to Harris (1992). Spines were categorized into four types: filopodia (protrusion with long neck and no

head), thin (protrusion with a neck and head $<0.6\,\mu m$ in diameter), stubby (protrusion with no obvious neck or head) or mushroom (protrusion with a neck and a head with a diameter $>0.6\,\mu m$). Dendritic spine analysis included spine density (number of spines/10 µm) and morphological classification. For each time-point, 10 dendritic segments per mice were analysed, corresponding to 600–1000 µm of dendritic branching by group ($n = 3$–5 mice). Detailed procedures for electron microscopy are described in the Supplementary material.

Electrophysiology

Hippocampal coronal slices (300-µm thick) were prepared from 3-month-old C57BL/6 mice and whole-cell patch-clamp recordings were performed from visually identified newborn cells using infrared and fluorescence video microscopy (Supplementary material).

Object location task

The object location task evaluates spatial hippocampal-dependent memory. This task addresses the ability of rodents to discriminate between a novel and a familiar spatial location. As previously described (Goodman *et al.*, 2010), the test takes place in a circular arena (50-cm diameter) containing a visual cue (rectangular striped pattern) and surrounded by a white curtain. One day before acquisition phase, each mouse is left for 10 min in the empty arena for familiarization (non-transgenic $n = 11$; APPxPS1 $n = 12$). The next day, two identical objects are placed in the middle of the arena. The mice are allowed to explore for 10 min during which the time spent exploring the two objects is recorded. In the test phase held 1 day later, identical copies of the sample objects are exposed and one of the two objects is moved to a novel location and mice are allowed to explore the objects during 10 min. The position (left or right) of the displaced object is chosen pseudo-randomly to reduce bias towards a particular position. The arena is cleaned thoroughly between trials to ensure the absence of olfactory cues. The same protocol but different objects were used for the second object location task (non-transgenic retrovirally-expressed (R)-GFP (R-GFP) $n = 5$; non-transgenic retrovirally-expressed (R)-*Neurod1* $n = 6$; APPxPS1 R-GFP $n = 6$; APPxPS1 R-*Neurod1* $n = 6$). Exploration was defined as directly attending to the object with the head no more than 2 cm from the object. Climbing over an object was considered as an explorative behaviour only when it was accompanied with sniffing of the object. The time spent exploring the displaced object during the test phase is expressed as a percentage of the exploration time of the displaced object related to the total exploration time for both objects (preference index).

Statistics

For all analyses, the observer was blind to the identity of the samples. First, Shapiro-Wilk tests were performed on each data set to test for distribution normality. Statistical analyses were run with Prism software (GraphPad 5.0). Data containing two experimental groups were analysed using the Student's *t*-test (parametric observations), Mann-Whitney test (non-parametric observations), one-way ANOVA test (more than two experimental conditions) and Wilcoxon matched pairs test (non-parametric paired observations). Statistical analyses on data containing more than two experimental groups were performed using two-way ANOVA test, followed by Bonferroni *post hoc* analyses, to account for multiple comparisons. Data are presented as mean ± SEM.

Results

Neurod1 and not *Neurog2* or *Neurod2*, directs exclusive differentiation of neural progenitors into neurons *in vivo*

The transcriptional cascade governing the generation of new neurons in the dentate gyrus includes the bHLH transcription factors *Neurog2*, *Neurod1* and *Neurod2*, which act in following the canonical pathway *Neurog2* → *Neurod1* → *Neurod2* (Roybon *et al.*, 2009; Hodge and Hevner, 2011). *In vitro*, the overexpression of each of these transcription factors is sufficient to direct exclusive neuronal commitment (Roybon *et al.*, 2009; Fedele *et al.*, 2011), but their respective role has not yet been examined in the adult brain. To determine which of these three factors displayed the greatest pro-neurogenic effect *in vivo*, they were expressed in adult hippocampal progenitors, using a Moloney Murine Leukemia Virus (MoMuLv) that specifically targets dividing cells (Zhao *et al.*, 2006).

Three-month-old wild-type mice received intra-hippocampal injections of retroviral vectors encoding the reporter gene for eGFP alone (control vector) or with each bHLH transcription factor (*Neurog2*, *Neurod1* or *Neurod2*) (Fig. 1A). Interestingly, 14 dpi, overexpression of *Neurod1*, but neither *Neurog2* nor *Neurod2*, was able to drive the exclusive production of new neurons in the adult hippocampus (Fig. 1). Animals injected with retrovirally-expressed (R)-*Neurog2*, retrovirally-expressed (R)-*Neurod2* or R-GFP vectors showed significant proportions of GFP+ cells that differentiated into astrocytes, whereas these cells were virtually absent following R-*Neurod1* injection (Fig. 1B and D).

Three weeks after viral injection, average numbers of GFP+ cells per brain were comparable between R-GFP and R-*Neurod1* groups (R-GFP: 1015.5 ± 167.2 GFP+ cells; R-*Neurod1*: 911.3 ± 129.4 GFP+ cells, $P > 0.05$, Fig. 1D). Thus, the size of the transduced cell population remained comparable between groups, despite variations inherent to viral injection. However, $68.2 \pm 4.3\%$ of the GFP+ cells expressed the neuronal marker NeuN after R-GFP injection, whilst this proportion reached $96.4 \pm 1.8\%$ among GFP+ cells transduced with R-*Neurod1* (Fig. 1C and D). Thus, *Neurod1* overexpression increased by ~25% the number of new granule neurons in the hippocampus at 21 dpi (R-GFP: 699.4 ± 127.7 GFP+/NeuN+ cells; R-*Neurod1*: 877.3 ± 119.3 GFP+/NeuN+ cells, Fig. 1D).

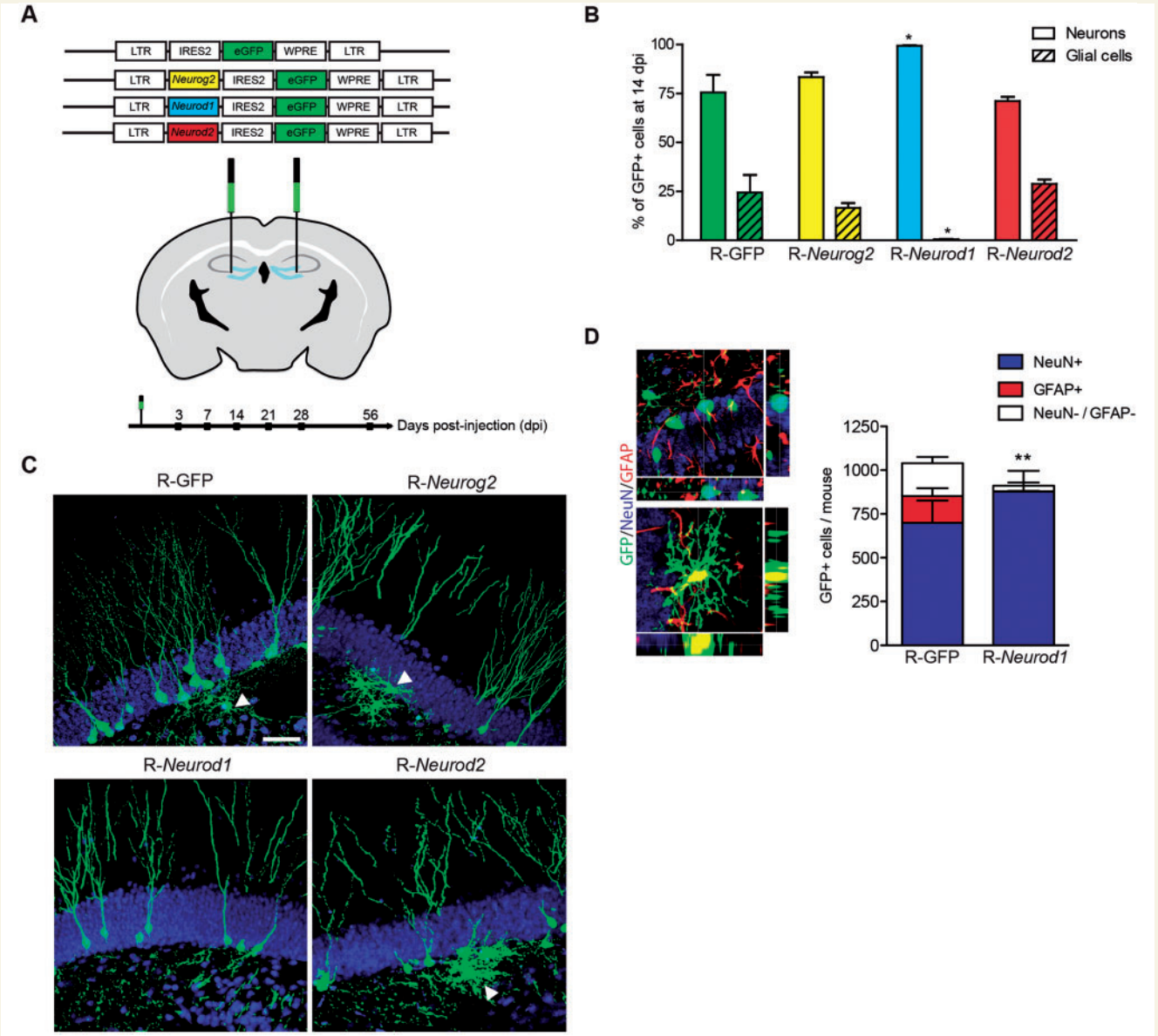

Figure 1 ***Neurod1* directs exclusive neuronal commitment of adult hippocampal progenitors *in vivo*.** (**A**) Schematic representation of the retroviral constructs used in this study and stereotaxic procedure for *in vivo* gene delivery. Experimental timeline indicating injections and time points studied. (**B**) Proportions of GFP+ cells expressing a glial or neuronal morphology 14 dpi of either R-GFP, R-*Neurog2*, R-*Neurod1* or R-*Neurod2* vector (n = 4–5 mice per group; $^{*}P < 0.05$, ANOVA). (**C**) Confocal micrographs of adult-born cells transduced by R-GFP, R-*Neurog2*, R-*Neurod1* or R-*Neurod2* vector (GFP: green, NeuN: blue), 21 days after viral injection. Scale bar = 50 μm. Transduced GFP+ cells display neuron or glial (arrows) morphologies. (**D**) Confocal micrographs of GFP+ cell expressing NeuN (*top*) and GFP+ cell expressing GFAP (*bottom*). Scale bar = 10 μm. Total number of GFP+ cells transduced per mouse brain, 21 days after injection of R-GFP or R-*Neurod1*-expressing vectors. Amongst GFP+ cells transduced with R-*Neurod1*, almost all cells expressed the neuronal marker NeuN (R-GFP: 699.4 ± 127.6 cells, R-*Neurod1*: 877.2 ± 119.3 cells, $P > 0.05$), whilst almost none of them expressed the astrocytic marker GFAP (R-GFP: 152.8 ± 44.9 cells, R-*Neurod1*; 2.8 ± 2.8 cells, $^{**}P < 0.01$).

Supporting these data and further providing functional evidence regarding these new neurons, patch-clamp recordings showed that 100% recorded GFP+ cells transduced with R-*Neurod1* expressed a response typical of neurons at 21 dpi (20 cells/20), whereas it was the case for only 66% of the GFP+ cells transduced with R-GFP (12 cells/18).

Neurod1 accelerates the morphological development of hippocampal new neurons

We next asked whether transduction with R-*Neurod1* influenced the integration of the new neurons in the

hippocampal network. Effective connectivity of granular neurons depends on their efferent output and afferent inputs (Zhao *et al.*, 2006), therefore we investigated the output of GFP+ neurons to the CA3 region by measuring their axonal length (Fig. 2A). As previously described (Zhao *et al.*, 2006), axonal length of GFP+ neurons increased substantially between 7 and 21 dpi among R-GFP transduced neurons (Supplementary Fig. 1). Remarkably at 14 dpi, axons from R-*Neurod1* neurons have travelled a greater distance towards CA3 than axons of age-matched R-GFP neurons (Fig. 2B). After 14 dpi, axons of R-*Neurod1* neurons do no grow significantly suggesting that at this time point, they have reached optimal location to establish synaptic contacts with CA3. In line with this idea, the majority of these GFP+ neurons have already migrated within the granular cell layer at 14 dpi (Supplementary Fig. 2) where they exhibit remarkably higher branching complexity and increased total dendritic length compared to R-GFP neurons (Fig. 2C–E). Altogether, these features suggest that R-*Neurod1* new neurons display a competitive advantage to receive inputs over R-GFP neurons or non-transduced new neurons of the same age.

Neurod1 stimulates synaptic connectivity and excitability of adult hippocampal new neurons

To evaluate the synaptic connectivity of GFP+ neurons, we analysed the density and shape of dendritic spines, a major site of functional glutamatergic inputs to the granular neurons (Esposito *et al.*, 2005). In agreement with Zhao *et al.* (2006), we found almost no dendritic spines on 14 dpi GFP+ neurons after R-GFP or R-*Neurod1* injection; however, they became clearly visible at 21 dpi (Fig. 3A and B). Spine density on control and R-*Neurod1* GFP+ neurons increased significantly between 21 and 56 dpi (Supplementary Fig. 3). Interestingly, at 21 dpi, R-*Neurod1* transduced neurons displayed higher density of dendritic spines than R-GFP neurons (Fig. 3B). Dendritic spines can be classified into four types based on their morphology: stubby, filopodia, thin and mushroom (Nimchinsky *et al.*, 2002; Sala, 2002) (Fig. 3C). At 21 dpi, increased densities of thin and mushroom-shaped spines were found on GFP+ neurons transduced with R-*Neurod1* compared to R-GFP (Fig. 3D). As thin and mushroom spines are typically more abundant in mature neurons (Nimchinsky *et al.*, 2002), our findings suggest a higher potential for synaptic integration of R-*Neurod1* neurons. Hence, R-*Neurod1* neurons at 21 dpi may be more prone to receive afferent cortical inputs and contribute to information encoding. To directly assess synapse formation, we performed electron microscopy and 3D reconstruction of GFP+ neurons. Mature synapses were identified on serial sections of 28 dpi R-*Neurod1* and R-GFP transduced neurons (Fig. 3E). As previously described (Toni *et al.*, 2008), dendritic spines with postsynaptic densities facing presynaptic boutons containing synaptic vesicles were observed, suggesting that despite their precocious development, spines on R-*Neurod1* neurons displayed ultrastructural criteria of mature synapses.

Lastly we sought to evaluate whether overexpression of *Neurod1* also regulates the physiological integration of new neurons within the hippocampal network. To be functionally relevant, new granule neurons must be able to generate action potentials and integrate afferent inputs. Previous reports have demonstrated that new neurons generate action potential in response to an excitatory drive when they reach 24–28 days of age (Mongiat *et al.*, 2009). Using whole-cell patch-clamp recordings in current clamp, we found that the maximal number of action potential that can be evoked by current steps at 21 dpi, was greater for R-*Neurod1* neurons than for R-GFP neurons (maximal number of action potential: R-GFP: 1.8 ± 0.6; R-*Neurod1*: 6.8 ± 1.7) (Fig. 4A and B). With time, new neurons receive increasing numbers of afferent terminals and consequently, the number of GFP+ cells responding to an extracellular stimulation of the granule cell layer also increases (Esposito *et al.*, 2005). In line with this, extracellular stimulation of the granular cell layer evoked postsynaptic currents in only 37.5% of R-GFP neurons at 21 dpi whereas the large majority (94%) of R-*Neurod1* GFP+ neurons responded to the stimulation (Fig. 4C). We confirmed the existence of functional GABAergic and glutamatergic inputs onto GFP+ neurons by evaluating the sensitivity of the recorded postsynaptic currents to ionotropic glutamate and $GABA_A$ receptor antagonists kynurenic acid and bicuculline, respectively. Evoked postsynaptic currents detected in R-*Neurod1* transduced GFP+ cells were completely abolished following successive treatment by these antagonists (Fig. 4D). This indicates that 21 dpi, R-*Neurod1* transduced GFP+ cells are able to integrate glutamatergic and GABAergic synaptic inputs and therefore are functional. Thus, new neurons overexpressing *Neurod1* are more easily excitable and consequently more susceptible to be recruited than control new neurons of the same age and pre-existing older neurons.

In summary, retrovirus-mediated expression of *Neurod1*directs adult endogenous hippocampal progenitors toward a neuronal fate, thus increasing the number of new neurons in the adult mouse brain. Potentializing this effect, new neurons overexpressing *Neurod1* are also endowed with a higher potential for connectivity and excitability, making them ideally suited to be involved in future memory processes. Thus, retroviral expression of *Neurod1* into mammalian neural progenitors *in vivo* may be particularly relevant in the context of pathologies associated with impaired differentiation of new neurons and spatial memory, as it is the case in Alzheimer's disease.

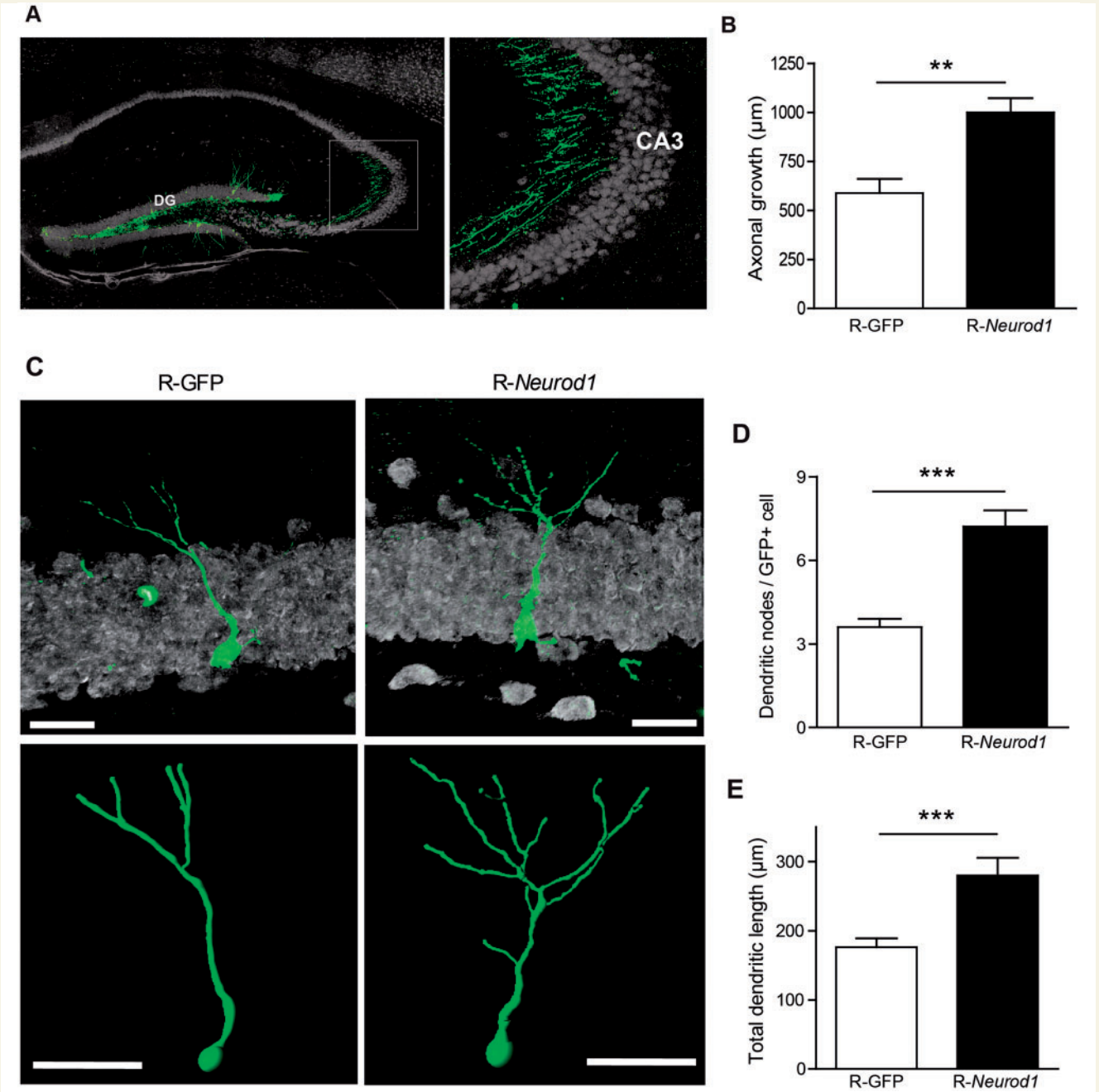

Figure 2 ***Neurod1* regulates the morphological development of new neurons.** (**A**) Axons of GFP+ neurons transduced with R-GFP extending into CA3 (enlargement, right). Scale bars = 300 µm; 100 µm. (**B**) At 14 dpi, axons of R-*Neurod1* GFP+ neurons have traveled a greater distance towards CA3, compared to GFP+ neurons. (**C**) Photographs and 3D reconstructions of 14 days post-injection GFP+ neurons transduced with R-GFP or R-*Neurod1*. Scale bar = 20 µm. More ramified (**D**) and longer (**E**) dendritic arbor in GFP+ neurons transduced with R-*Neurod1* compared to R-GFP at 14 dpi, (n = 4–5 mice/group, $^{**}P < 0.01$; $^{***}P < 0.001$, t-test).

Enhanced functional integration of new neurons alleviates memory deficits in a mouse model of Alzheimer's disease

Alzheimer's disease is characterized by age-related memory and cognitive impairments. In several Alzheimer's disease mouse models (Verret *et al.*, 2007; Krezymon *et al.*, 2013) and in patients with Alzheimer's disease (Jin *et al.*, 2004; Li *et al.*, 2008), alterations of hippocampal neurogenesis that concern maturation and differentiation of neural progenitor cells have been described (Lazarov and Demars, 2012). As new hippocampal neurons contribute to spatial memory processes in the healthy mouse brain (Deng *et al.*, 2010), supplying the Alzheimer's disease brain with

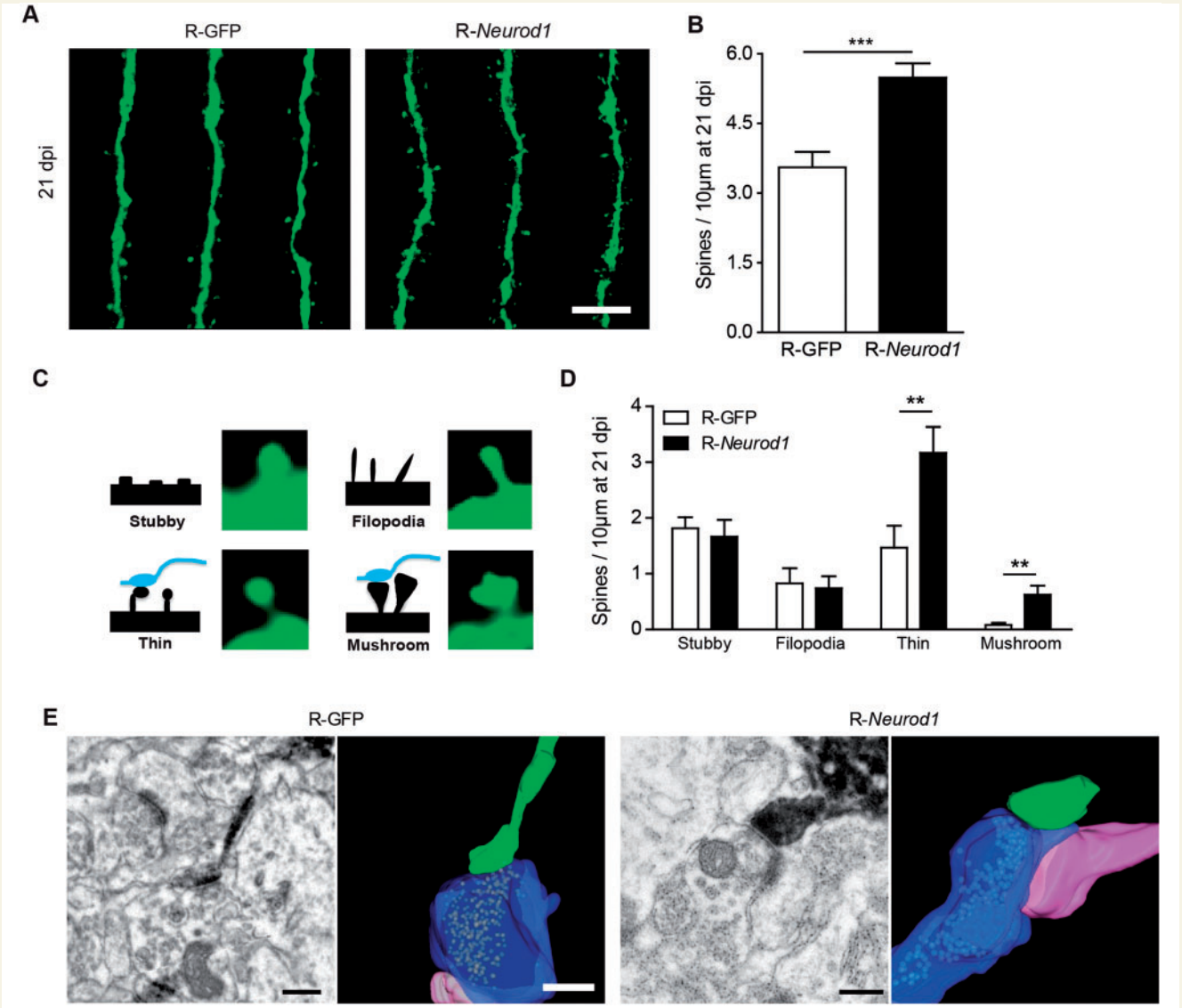

Figure 3 *Neurod1* promotes the formation of mature dendritic spines on new neurons. (**A**) Confocal projections of dendrites of GFP+ neurons transduced with R-GFP or R-*Neurod1* at 21 dpi. Scale bar = 5 µm. (**B**) At 21 dpi, GFP+ neurons transduced with R-*Neurod1* exhibit significantly more spines than GFP+ neurons transduced with R-GFP (R-GFP $n = 404$ spines, R-*Neurod1*: $n = 648$ spines, $^{***}P < 0.001$). (**C**) Illustration depicting different spine subtypes based on their morphology. (**D**) At 21 dpi, GFP+ neurons transduced with R-*Neurod1* display higher densities of thin spines (R-GFP $n = 143$ thins, R-*Neurod1* $n = 338$ thins; $^{**}P < 0.01$, unpaired *t*-test) and mushroom spines (R-GFP $n = 21$ mushrooms, R-*Neurod1* $n = 51$ mushrooms, $^{**}P < 0.01$, unpaired *t*-test) compared to R-GFP transduced neurons. (**E**) At 28 dpi, dendritic spines on neurons transduced with R-GFP or R-*Neurod1* display a similar ultrastructure, typical of functional spines, as evidenced by the presence of a postsynaptic density and numerous docked vesicles. Electron micrographs (*left*) and 3D reconstructions (*right*) of axo-spinous synapses from GFP+ neurons transduced with R-GFP or R-*Neurod1* after GFP immunostaining (green: GFP+ spines; pink: spines not labelled with GFP; blue: axonal bouton; yellow: synaptic vesicles). Scale bars = 0.2 µm.

highly excitable new granule neurons might improve hippocampal cognitive function.

To test this possibility, we applied retroviral delivery of *Neurod1* to the APPxPS1 mouse model of Alzheimer's disease which displays impaired memory (Puoliväli *et al.*, 2002; Gallagher *et al.*, 2013) and altered hippocampal neurogenesis (Verret *et al.*, 2007; Demars *et al.*, 2010). APPxPS1 of middle age and age-matched non-transgenic mice were tested before and after R-*Neurod1* administration in two independent object location tasks (Fig. 5A). This task was chosen because it implies changes in the metric spatial relations between similar objects and therefore relies on dentate gyrus-dependent spatial pattern separation processes (Hunsaker *et al.*, 2009; Kannangara *et al.*, 2014). The contribution of new granule neurons to spatial pattern separation was recently evidenced by a number of elegant studies (Clelland *et al.*, 2009; Creer *et al.*, 2010; Sahay *et al.*, 2011; Niibori *et al.*, 2012) and is further supported by our own data

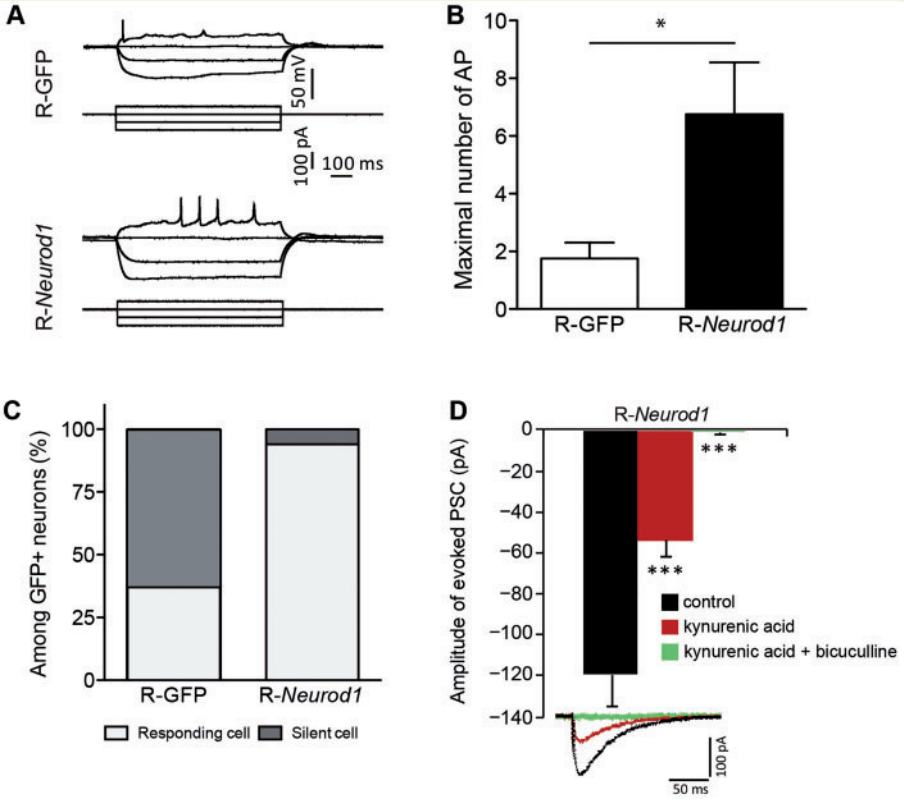

Figure 4 Functional integration of new neurons is improved by *Neurod1*. (**A**) Electrophysiological behaviour of GFP+ neurons 21 days after transduction with R-GFP or R-*Neurod1*. Voltage-responses induced by current injections: −100 to 0 pA by increments of 50 pA. (**B**) Maximal number of action potentials (AP) generated during current injection steps (number of recorded cells at 21 dpi: R-GFP = 12; R-*Neurod1* = 20; $^{*}P < 0.05$, *t*-test). (**C**) Percentage of GFP+ neurons responding to an extracellular electrical stimulation of the granule cell layer. A neuron was considered to be silent when it did not respond to a 1.2 mA stimulation while one adjacent granule cell did (responding cells at 21 dpi: R-GFP 3/8, R-*Neurod1* 15/16). (**D**) Amplitude of postsynaptic current (PSC) evoked in *Neurod1*-transduced neurons by extracellular stimulation of the granule cell layer (pA) at 21 dpi ($n = 8$). Traces illustrate examples of evoked postsynaptic current in standard conditions (black), after application of kynurenic acid (a glutamate receptor antagonist) alone (red), or together with bicuculline (a $GABA_A$ receptor antagonist) (green) ($^{***}P < 0.001$, paired *t*-test).

showing that in our hands, the object location protocol is sensitive to hippocampal neurogenesis depletion (Goodman *et al.*, 2010). During the acquisition phase held before viral administration, non-transgenic and APPxPS1 mice spent the same amount of time exploring the objects (Supplementary Fig 4A), indicating that mice from both genotypes exhibited the same exploratory drive. For each genotype, mice were randomly divided into two groups, which would later receive either control R-GFP or R-*Neurod1* vector. During memory testing 24 h later, the two groups of non-transgenic mice explored preferentially the object that had been moved to a novel location ($P = 0.008$; $P = 0.01$ before injection of R-GFP or R-*Neurod1*, respectively) (Fig. 5B). In contrast, both groups of APPxPS1 mice showed no exploratory preference for the displaced object ($P = 0.38$; $P = 0.54$, Fig. 5B) indicating that Alzheimer's disease mice were unable to discriminate the novel from the familiar location. These transgenic mice therefore provide a robust animal model in which a rescuing effect mediated by *Neurod1* on cognitive impairment can be interrogated.

To do so, animals were submitted to the same memory task using new objects, 21 days after retroviral injection (Fig. 5A), corresponding to the time when *Neurod1* transduced new neurons are endowed with enhanced potential for connectivity and excitability (Figs 1–4). During the exploration phase, R-GFP and R-*Neurod1* mice spent the same amount of time exploring each object ($P > 0.05$, Supplementary Fig 4B), indicating that viral administration did not impact the interest of the mice for the objects.

During memory testing, 1 day later, non-transgenic mice injected with R-GFP explored preferentially the displaced object ($P < 0.01$) and it was also the case of non-transgenic mice after R-*Neurod1* injection ($P < 0.05$). In contrast, APPxPS1 mice injected with R-GFP showed no preference for any of the objects ($P > 0.05$, Fig. 5B). Remarkably, this memory impairment was abolished following R-*Neurod1* injection as APPxPS1 mice explored significantly more the displaced object ($P < 0.01$, Fig. 5B), indicating that they were now able to discriminate the novel location from the familiar one. Finally, paired *t*-test analysis comparing spatial memory

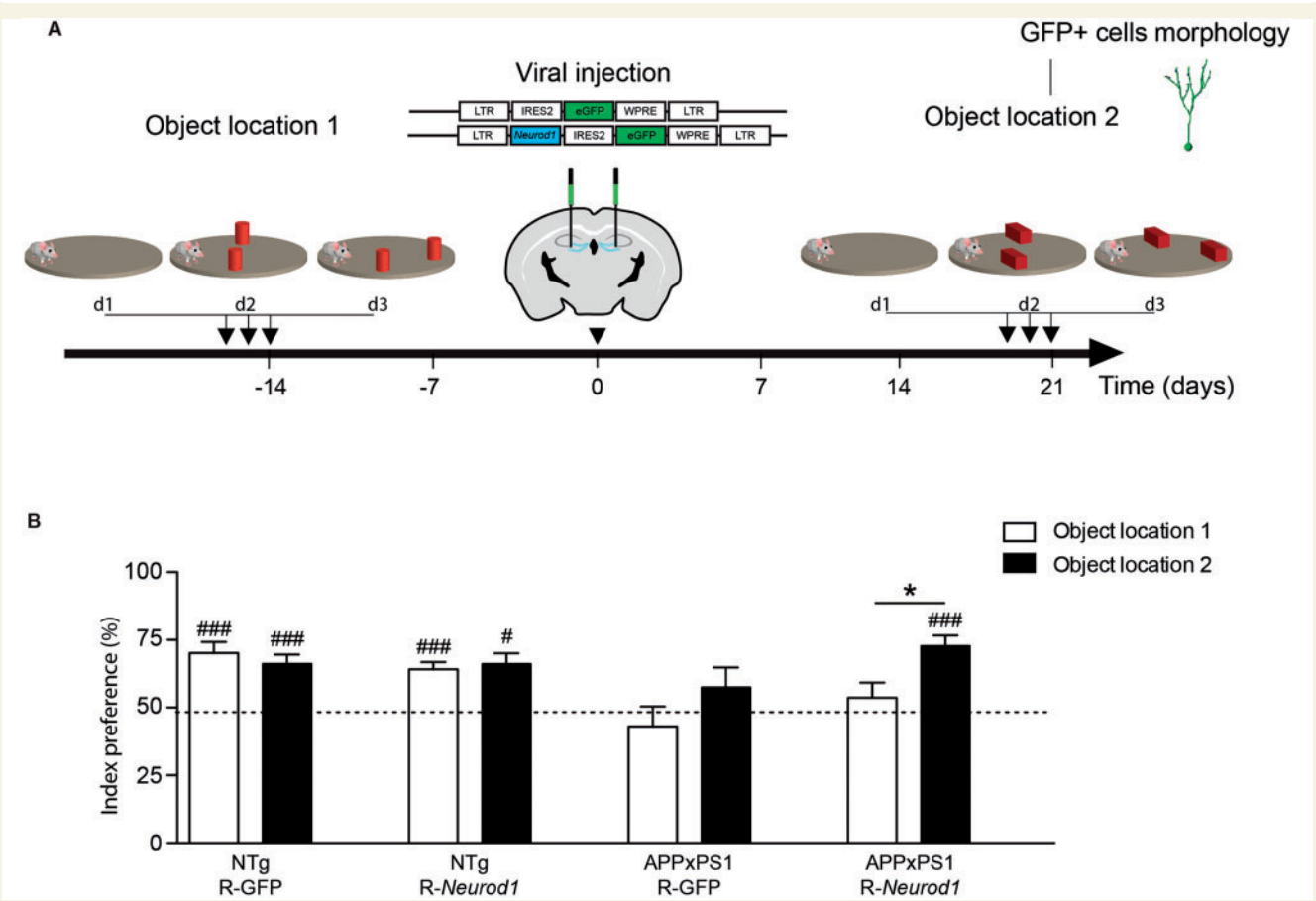

Figure 5 Rescue of spatial memory deficits in a mouse model of Alzheimer's disease. (**A**) Experimental timeline. (**B**) Memory performances in the object location tasks before (white bars) and after (black bars) viral injection. Before injection, APPxPS1 mice show impaired spatial memory. Memory deficit in APPxPS1 mice is abolished 21 days after the injection of R-*Neurod1*, but not R-GFP. Horizontal dotted line represents chance level (non-transgenic R-GFP $n = 5$; non-transgenic R-*Neurod1* $n = 6$; APPxPS1 R-GFP $n = 6$; APPxPS1 R-*Neurod1* $n = 6$; $^{###}P < 0.001$; $^{\#}P < 0.05$ index versus chance level 50%, Wilcoxon signed-rank test; $^{*}P < 0.05$ Wilcoxon matched pairs test). NTg = non-transgenic.

of the same mice before and after viral vector injection further confirmed that APPxPS1 mice had improved their performances 21 days after neural hippocampal progenitors were transduced with R-*Neurod1* (before injection: 53.6 ± 5.6%, after injection: 72.7 ± 4.0%; $P < 0.05$, Fig. 5B).

At the cellular level, new neurons in the population of GFP+ cells were quantified based on their typical morphology (Fig. 6A). Significantly fewer new neurons were found in the hippocampus of middle age APPxPS1 compared to age-matched non-transgenic mice 21 days after R-GFP injection (non-transgenic: 91.7 ± 17.23 neurons, APPxPS1: 21.8 ± 9.0 neurons; $P < 0.05$, Fig. 6B). These findings are in line with previously reported impairment of adult hippocampal neurogenesis in APPxPS1 mice using bromodeoxyuridine (BrdU) labelling (Hamilton and Holscher, 2012). As a means to estimate the connectivity of these new neurons, we evaluated their dendritic spine density (Fig. 6C). Moreover, new neurons in APPxPS1 mice exhibited reduced spine density compared to neurons in non-transgenic mice (after R-GFP: 2.4 ± 0.4 versus 5.3 ± 0.4 spines/10 μm, respectively; $P < 0.001$) (Fig. 6D). After R-*Neurod1* administration, numbers of GFP+ new neurons increased in both genotypes, but this increase remained below significance (Fig. 6B). However, R-*Neurod1* induced a remarkable 2-fold increase of spine density on APPxPS1 new neurons (2.4 ± 0.4 versus 5.7 ± 0.4 spines/10 μm; $P < 0.001$), which thus reached similar spine density than non-transgenic neurons (5.7 ± 0.4 versus 5.0 ± 0.4 spines/10 μm; $P > 0.05$, Fig. 6C and D). Thus, retroviral delivery of *Neurod1* in aged Alzheimer's disease mice triggers the production of new hippocampal neurons bearing a high potential for synaptic integration and sufficient to rescue spatial memory.

Discussion

Here, we provide for the first time evidence that single gene delivery of a bHLH transcription factor selectively into neural stem/progenitor cells of the adult hippocampus

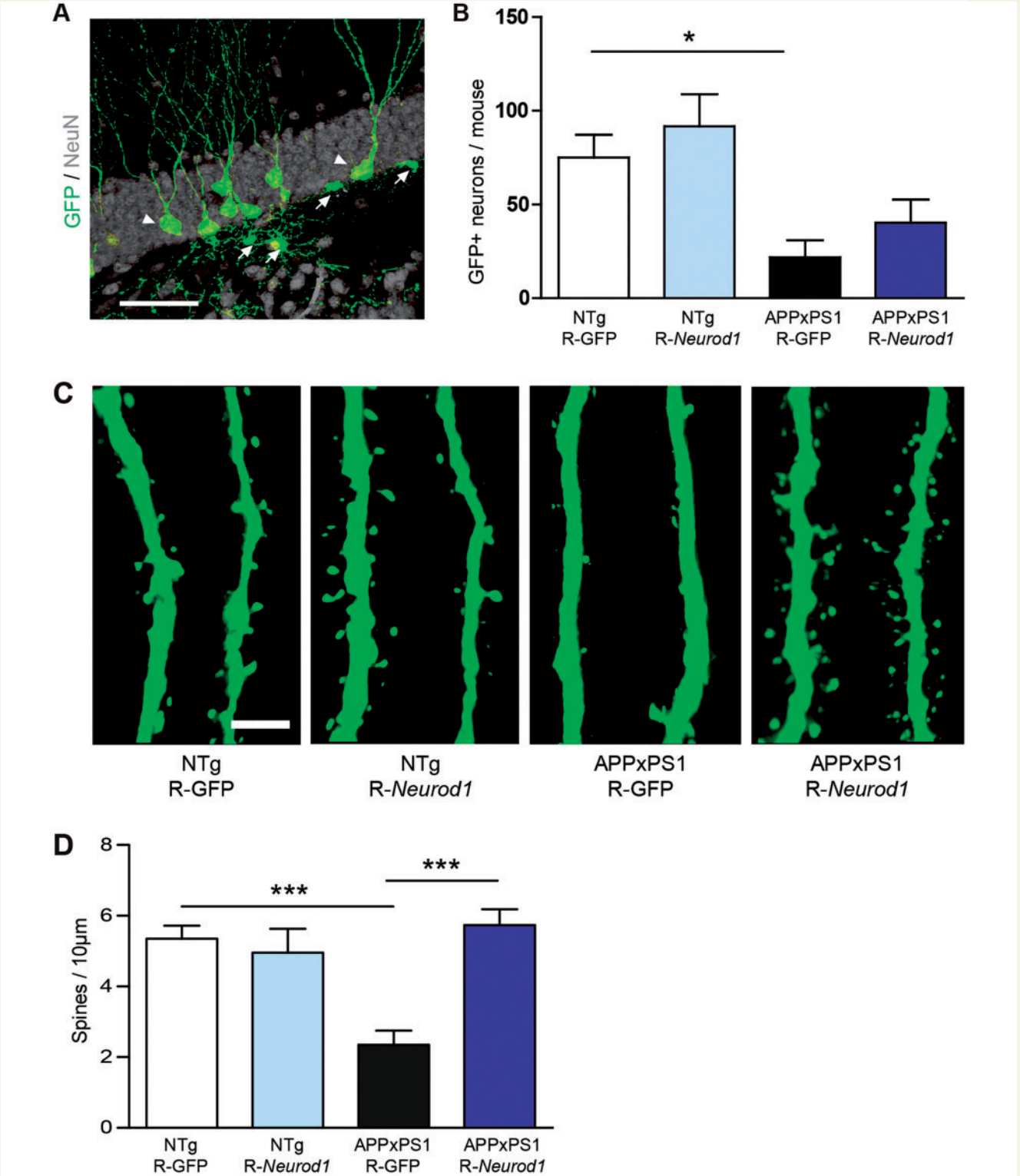

Figure 6 ***Neurod1* rescues dendritic spines on new neurons in Alzheimer's disease mice.** (**A**) Photomicrograph of GFP+ cells expressing neuronal (arrowheads) or glial (arrows) morphologies in a non-transgenic mouse, 21 days after R-GFP injection. Scale bar = 50 µm. (**B**) Absolute numbers of GFP+ neurons per mouse brain, 21 days after injection of R-GFP or R-*Neurod1*-expressing vectors. Fewer new neurons are generated in APPxPS1 mice compared to non-transgenic (two-way ANOVA and Bonferroni post-tests, $^{*}P < 0.05$). Transduction with R-*Neurod1* was not sufficient to increase the number of new neurons in the Alzheimer's disease mice. (**C**) Dendritic segments from GFP+ neurons, 21 days after injection of R-GFP or R-*Neurod1* in non-transgenic or APPxPS1 mice. Scale bar = 5 µm. (**D**) In control conditions, new neurons in APPxPS1 exhibited significantly less protrusions than in non-transgenic mice (non-transgenic R-GFP $n = 291$ spines, APPxPS1 R-GFP $n = 148$ spines, $n = 3$–4 mice/group, two-way ANOVA $^{***}P < 0.001$). R-*Neurod1* rescued spine density in new neurons of APPxPS1 mice (APPxPS1 R-GFP $n = 148$ spines, APPxPS1 R-*Neurod1* $n = 299$ spines, $n = 3$–4 mice/group, two-way ANOVA, $^{***}P < 0.001$).

in vivo, enhances neuronal fate, maturation and synaptic integration. We applied such gene-targeting strategy to a mouse model Alzheimer's disease, revealing its potential to abolish hippocampal-dependent memory deficits.

The transcriptional programs underlying the generation of mature functional neurons from neural stem cells in the adult hippocampus have not been fully elucidated yet. However, during embryonic neurogenesis, the critical role of cell-intrinsic bHLH factors has been well demonstrated (Guillemot, 2007). Among the three bHLH transcription factors studied (*Neurog2*, *Neurod1*, *Neurod2*), only *Neurod1* showed the potential to direct exclusive neuronal commitment of adult hippocampal neural progenitor cells in young wild-type mice (Gao *et al.*, 2009). In the middle age brain, *Neurod1* has no effect on cell fate choice, suggesting that pathways triggered by *Neurod1* may be affected by age-related brain changes. This effect on neuronal fate correlates with the reported transient expression of *Neurod1* gene during hippocampal neurogenesis; whereas early stages of hippocampal neurogenesis are controlled in part by *Neurog2*, late ones, including final differentiation and maturation of neural progenitors into neurons, are under the control of *Neurod1* and *Neurod2* (Roybon *et al.*, 2009). *Neurod1* is also involved in the generation and maintenance of dendrites (Gaudilliere *et al.*, 2004) and required for the survival of the newborn neurons in the dentate gyrus (Miyata *et al.*, 1999; Gao *et al.*, 2009; Kuwabara *et al.*, 2009). Further extending these data, we report that *Neurod1* expression in adult neural progenitor cells, accelerates the timing of their differentiation into functional neurons.

Discovery in the adult brain of neural progenitor cells with a capacity to self-renew has indeed raised interest for their use to treat neurodegenerative diseases such as Alzheimer's disease. Only few studies have been published to date regarding adult neurogenesis in the human Alzheimer's disease brain. Although these reports seem to provide conflicting data, they converge nonetheless to indicate that endogenous proliferative activity persists in the dentate gyrus of patients with Alzheimer's disease although it does not produce functional neurons to overcome neuronal loss (Jin *et al.*, 2004; Boekhoorn *et al.*, 2006; Li *et al.*, 2008). Similarly, hippocampal cell proliferation persists in several Alzheimer's disease transgenic mouse models and is also followed by impaired differentiation or maturation of news neurons early during disease development, resulting in altered production of new neurons (Rodríguez *et al.*, 2008; Hamilton *et al.*, 2010; Krezymon *et al.*, 2013). At middle age, the APPxPS1 mice used in the present study display spatial memory deficits and impaired production of new hippocampal neurons (Verret *et al.*, 2007; Gallagher *et al.*, 2013) which display strongly altered spine density. Deleterious effects of amyloid-β oligomers accumulation at the synapse have been reported in several mouse models of Alzheimer's disease, as well as in patients with Alzheimer's disease (Takahashi *et al.*, 2004; Lacor *et al.*, 2007; Wilcox *et al.*, 2011), suggesting that elevated brain levels of amyloid-β oligomers present in our APPxPS1 mice at middle age (Gallagher *et al.*, 2013) may contribute to these dendritic spine alterations.

Given the persisting proliferative activity in the dentate gyrus of APPxPS1 mice at middle age, it appeared relevant to target these dividing cells in an attempt to stimulate adult neurogenesis. Remarkably, *Neurod1* expression into dividing neural stem cells of APPxPS1 mice allowed new neurons to reach terminal stages of their differentiation and abolished memory deficits, without attenuating hallmarks of neuropathology. Our findings are in line with recent evidence pointing out that oligomeric forms of amyloid rather than amyloid plaques are critical for the functional deficits observed in Alzheimer's disease (Lesné *et al.*, 2006; Cavallucci *et al.*, 2012).

These data raise questions regarding how new neurons can significantly influence memory processing? Accumulating evidence has demonstrated that manipulation of adult neurogenesis impacts learning and memory performances in several hippocampal-dependent tasks (Greenough *et al.*, 1999; Deng *et al.*, 2010). Although the specific contribution of new neurons to memory processes is still debated, theoretical models, along with experimental data, suggest that adult born granule cells in the dentate gyrus may contribute to pattern separation and could be required for the memorization and/or the recall of spatial relationships between objects (Deng *et al.*, 2010; Sahay *et al.*, 2011). Here, we used the object location task where the mice have to discriminate between fine spatial changes. The ability for pattern separation, a processes by which closely related memories are encoded separately in the hippocampus, has been shown to request intact dentate gyrus and intact adult neurogenesis (Deng *et al.*, 2010; Sahay *et al.*, 2011). Theoretical approaches have suggested that immature neurons represent a population of broadly tuned neurons, ideally fitted to exert a significant functional influence on the network and to make a distinct contribution to the separation properties of the dentate gyrus (Aimone *et al.*, 2009, 2010). Supporting these predictions, it was described that new neurons go through a time-window, between the third and fourth week after their birth, when they show increased intrinsic excitability and enhanced plasticity (Schmidt-Hieber *et al.*, 2004; Esposito *et al.*, 2005; Ge *et al.*, 2007) and can be preferentially recruited upon hippocampal activation (Jessberger and Kempermann, 2003; Bruel-jungerman *et al.*, 2006). In contrast to the study by Fitzsimons *et al.* (2013), which shows accelerated new neuron migration and maturation after glucocorticoid receptor knockdown, in our work, *Neurod1* overexpression did not induce ectopic positioning of new neurons in APPxPS1 mice (Supplementary Fig. 5). However, in these mice, *Neurod1* overexpression increased the structural maturation of new neurons, potentially enhancing their probability to be activated by entorhinal afferents. Newborn granule cells also receive transient afferents from intra-hippocampal cells including mature granule cells (Vivar *et al.*, 2012). Such substantial connectivity between

mature and newborn granule cells during the first month of their development might facilitate activity-dependent maturation of new granule cells. In APPxPS1 mice, electron microscopic evidence show synaptic changes in plaque-free regions of the brain, suggesting that synaptic alterations are widespread in this animal model (Alonso-Nanclares *et al.*, 2013). These findings support the actual view that oligomeric forms of amyloid, rather than amyloid plaques, are key players of Alzheimer's disease physiopathology (Lesné *et al.*, 2006; Cavallucci *et al.*, 2012). Whether altered monosynaptic inputs from mature granule cells contribute to the impaired integration of adult-born neurons, and whether *Neurod1* overexpression is beneficial, remains to be determined.

APPxPS1 mice were submitted to memory testing precisely during the critical period of new neuron maturation, when they display a low input specificity and are more easily activated than other pre-existing neurons in wild-type mice (Marín-Burgin and Schinder, 2012). Therefore, the relative contribution of new neurons to dentate gyrus function is most likely high at this stage. Future experiments designed to specifically inactivate *Neurod1* expressing neurons in APPxPS1 mice might provide insights into their specific contribution to memory improvement. In line with this, recent work demonstrated that changes in the differentiation rate of new neurons greatly impact animal's cognitive performances (Farioli-Vecchioli *et al.*, 2008, 2009). Predictions from these data indicate that in pathologies, which like Alzheimer's disease are characterized by memory impairments and deficits of the maturation and differentiation of neural progenitor cells (Lazarov and Demars, 2012), the correct timing of neuron differentiation may be a critical variable to consider (Tirone *et al.*, 2013). Our findings of enhanced neuronal differentiation paralleled with rescued hippocampal-dependent memory performances in Alzheimer's disease mice, support this prediction.

In contrast to our data in young healthy mice, *Neurod1* did not significantly increase the number of new neurons in older non-transgenic mice. Therefore, one may wonder how a relatively small population of new neurons is able to impact brain cognitive function? Although it is not yet known how many neurons are required to drive memory processes, the recent study by Gu *et al.* (2012) elegantly showed that controlling the activity of a group of ~1700 new neurons in young mice is sufficient to substantially influence hippocampal-dependent memory retrieval. In middle age APPxPS1 mice, only few new granule cells integrate the hippocampus in basal conditions and previous studies suggest that this deficit of neurogenesis builds on from young age in these mice (Verret *et al.*, 2007; Demars *et al.*, 2010; Hamilton and Holscher, 2012). Retrovirally-mediated expression of *Neurod1* drove the production of a pool of highly connected and potentially recruitable new neurons. Although sparse, these new neurons convey the potential to substantially expand the plasticity of APPxPS1 mice dentate gyrus and thereby are able to restore spatial memory abilities in these animals. Hence, our data suggest that only a discrete number of new granule neurons is necessary for the encoding of spatial information in the object location task. Supporting this idea and consistent with the sparse encoding typical of the dentate gyrus, we and others have reported that only a small proportion of a given population of immature neurons is activated upon efficient spatial memory retrieval (Tashiro *et al.*, 2007; Trouche *et al.*, 2009).

In the context of Alzheimer's disease, another crucial point is the capacity of new neurons for synaptic integration in the dentate gyrus, independent of their number. Dendritic spines are the main targets of excitatory synapses in the mammalian cortex. Therefore, increasing spine density on new neurons via *Neurod1* overexpression, provides these neurons with a higher potential for synaptic integration into the network. Supporting this idea, we found that *Neurod1*-transduced neurons in the brain of healthy mice were more prone to generate action potentials and integrate afferent inputs. Unfortunately, the sparse number of new neurons prevented us from addressing this question in APPxPS1 mice. Recently, Seib *et al.* (2013) showed that loss of the Wnt antagonist DKK1 in neural progenitors led to increased dendritic complexity of new neurons, whereas mice deficient for DKK1 displayed enhanced spatial memory. Conversely, the reduction of dendritic arborization and spine density of new hippocampal neurons upon conditional expression of *PC3* gene (now known as *Btg2*) led to impaired contextual fear memory (Farioli-Vecchioli *et al.*, 2008). These data, together with ours, support the idea that increasing dendritic and spine complexity of newborn neurons is a means to enhance hippocampal-dependent memory performances without changing their overall number.

In conclusion, our data reveal that manipulating the connectivity of adult hippocampal neural progenitors *in vivo*, by forced expression of single transcription factor *Neurod1*, may open new avenues for the treatment of neurodegenerative diseases associated with hippocampal dysfunction.

Acknowledgements

We thank H. Halley for breeding and genotyping the APPxPS1 mice, M. Alonzo, M.E. Marsan, M. Zerwas and B. Robert for their technical help and Drs G.K. Gouras, F. Pituello, L. Verret, C. Florian and A.F. Schinder for their helpful comments and discussions on the manuscript. APP and PS1 mice founders were graciously provided by Dr J.L. Jankowsky. Mice were housed in the ABC Facility of ANEXPLO Toulouse. Confocal images were acquired at the TRI Imaging Facility in Toulouse, France and electron microscopy images were acquired at the electron microscopy facility of the University of Lausanne, Switzerland.

Funding

This work was supported by Association France Alzheimer (FA2010 to C.R. and T.G.), Fédération pour la Recherche sur le Cerveau (AOFRC2009 to C.R.) and Region Midi-Pyrénées (APRRTT2010 to C.R.), Kung Fysiografiska Sällskapet, The Crafoord Foundation and MultiPark (to L.R.), and the Swiss National Science Foundation (to N.T.). K. Richetin was supported by the French Ministry of Research and an ATUPS travel grant. C. Leclerc was supported by France Alzheimer Association.

Supplementary material

Supplementary material is available at *Brain* online.

References

Aimone JB, Deng W, Gage FH. Adult neurogenesis: integrating theories and separating functions. Trends Cogn Sci 2010; 14: 325–37.

Aimone JB, Deng W, Gage FH. Resolving new memories: a critical look at the dentate gyrus adult neurogenesis and pattern separation. Neuron 2011; 70: 589–96.

Aimone JB, Wiles J, Gage FH. Computational influence of adult neurogenesis on memory encoding. Neuron 2009; 61: 187–202.

Alonso-Nanclares L, Merino-Serrais P, Gonzalez S, DeFelipe J. Synaptic changes in the dentate gyrus of APP, PS1 transgenic mice revealed by electron microscopy. J Neuropathol Exp Neurol 2013; 72: 386–95.

Altman J, Das GD. Autoradiographic and histological evidence of postnatal hippocampal neurogenesis in rats. J Comp Neurol 1965; 124: 319–35.

Boekhoorn K, Joels M, Lucassen PJ. Increased proliferation reflects glial and vascular-associated changes but not neurogenesis in the presenile Alzheimer hippocampus. Neurobiol Dis 2006; 24: 1–14.

Bruel-jungerman E, Davis S, Rampon C, Laroche S. Long-term potentiation enhances neurogenesis in the adult dentate gyrus. J Neurosci 2006; 26: 5888–93.

Cavallucci V, D'Amelio M, Cecconi F. Aβ toxicity in Alzheimer's disease. Mol Neurobiol 2012; 45: 366–78.

Clelland CD, Choi M, Romberg C, Clemenson GD, Fragniere A, Tyers P, et al. A functional role for adult hippocampal neurogenesis in spatial pattern separation. Science 2009; 325: 210–13.

Coras R, Siebzehnrubl FA, Pauli E, Huttner HB, Njunting M, Kobow K, et al. Low proliferation and differentiation capacities of adult hippocampal stem cells correlate with memory dysfunction in humans. Brain 2010; 11: 3359–72.

Creer DJ, Romberg C, Saksida LM, van Praag H, Bussey TJ. Running enhances spatial pattern separation in mice. Proc Natl Acad Sci USA 2010; 107: 2367–72.

Demars M, Hu YS, Gadadhar A, Lazarov O. Impaired neurogenesis is an early event in the etiology of familial Alzheimer's disease in transgenic mice. J Neurosci Res 2010; 88: 2103–17.

Deng W, Aimone JB, Gage FH. New neurons and new memories: how does adult hippocampal neurogenesis affect learning and memory? Nat Rev Neurosci 2010; 11: 339–50.

Ekonomou A, Savva GM, Brayne C, Forster G, Francis PT, Johnson M, et al. Stage-specific changes in neurogenic and glial markers in Alzheimer's disease. Biol Psychiatry 2014; 1–8.

Eriksson PS, Perfilieva E, Bjork-Eriksson T, Alborn AM, Nordborg C, Peterson DA, et al. Neurogenesis in the adult human hippocampus. Nat Med 1998; 4: 1313–17.

Esposito MS, Piatti VC, Laplagne DA, Morgenstern A, Ferrari CC, Pitossi FJ, et al. Neuronal differentiation in the adult hippocampus recapitulates embryonic development. J Neurosci 2005; 25: 10074–86.

Farioli-Vecchioli S, Saraulli D, Costanzi M, Leonardi L, Cinà I, Micheli L, et al. Impaired terminal differentiation of hippocampal granule neurons and defective contextual memory in PC3, Tis21 knockout mice. PLoS One 2009; 4: e8339.

Farioli-Vecchioli S, Saraulli D, Costanzi M, Pacioni S, Cinà I, Aceti M, et al. The timing of differentiation of adult hippocampal neurons is crucial for spatial memory. PLoS Biol 2008; 6: 2188–204.

Fedele V, Roybon L, Nordström U, Li JY, Brundin P. Neurogenesis in the R6, 2 mouse model of Huntington's disease is impaired at the level of Neurod1. Neuroscience 2011; 173: 76–81.

Fiorentini A, Rosi MC, Grossi C, Luccarini I, Casamenti F. Lithium improves hippocampal neurogenesis neuropathology and cognitive functions in APP mutant mice. PLoS One 2010; 5: e14382.

Fitzsimons CP, van Hooijdonk LW, Schouten M, Zalachoras I, Brinks V, Zheng T, et al. Knockdown of the glucocorticoid receptor alters functional integration of newborn neurons in the adult hippocampus and impairs fear-motivated behavior. Mol Psychiatry 2013; 18: 993–1005.

Gallagher JJ, Minogue M, Lynch M. Impaired performance of female APP, PS1 mice in the Morris water maze is coupled with increased Aβ accumulation and microglial activation. Neurodegener Dis 2013; 11: 33–41.

Gao Z, Ure K, Ables JL, Lagace DC, Nave KA, Goebbels S, et al. Neurod1 is essential for the survival and maturation of adult-born neurons. Nat Neurosci 2009; 12: 1090–2.

Gaudilliere B, Konishi Y, de la Iglesia N, Yao G, Bonni AA. CaMKII-NeuroD signaling pathway specifies dendritic morphogenesis. Neuron 2004; 41: 229–41.

Ge S, Yang CH, Hsu KS, Ming GL, Song H. A Critical period for enhanced synaptic plasticity in newly generated neurons of the adult brain. Neuron 2007; 54: 559–66.

Gomez-Nicola D, Suzzi S, Vargas-Caballero M, Fransen NL, Al-Malki H, Cebrian-Silla A, et al. Temporal dynamics of hippocampal neurogenesis in chronic neurodegeneration. Brain 2014; 2312–28.

Goodman T, Trouche S, Massou I, Verret L, Zerwas M, Roullet P, et al. Young hippocampal neurons are critical for recent and remote spatial memory in adult mice. Neuroscience 2010; 171: 769–78.

Greenough WT, Cohen NJ, Juraska JM. New neurons in old brains: learning to survive? Nat Neurosci 1999; 2: 203–5.

Gu Y, Arruda-Carvalho M, Wang J, Janoschka SR, Josselyn S, Frankland PW, et al. Optical controlling reveals time-dependent roles for adult-born dentate granule cells. Nat Neurosci 2012; 15: 1700–6.

Guillemot F. Cell fate specification in the mammalian telencephalon. Prog Neurobiol 2007; 83: 37–52.

Hamilton A, Holscher C. The effect of ageing on neurogenesis and oxidative stress in the APP (swe), PS1 (deltaE9) mouse model of Alzheimer's disease. Brain Res 2012; 1449: 83–93.

Hamilton LK, Aumont A, Julien C, Vadnais A, Calon F, Fernandes KJL. Widespread deficits in adult neurogenesis precede plaque and tangle formation in the 3xTg mouse model of Alzheimer's disease. Eur J Neurosci 2010; 32: 905–20.

Harris M. Three-dimensional structure of dendritic spines and synapses rat hippocampus (CA1) at postnatal day 15 and adult ages: implications for the maturation of synaptic physiology and long-term potentiation. J Neurosci 1992; 12: 2685–705.

Hodge RD, Hevner RF. Expression and actions of transcription factors in adult hippocampal neurogenesis. Dev Neurobiol 2011; 71: 680–9.

Hofstetter CP, Holmström NAV, Lilja JA, Schweinhardt P, Hao J, Spenger C, et al. Allodynia limits the usefulness of intraspinal neural stem cell grafts; directed differentiation improves outcome. Nat Neurosci 2005; 8: 346–53.

Hunsaker MR, Wenzel HJ, Willemsen R, Berman RF. Progressive spatial processing deficits in a mouse model of the fragile X premutation. Behav Neurosci 2009; 123: 1315–24.

Jankowsky JL, Fadale DJ, Anderson J, Xu GM, Gonzales V, Jenkins NA, et al. Mutant presenilins specifically elevate the levels of the 42 residue beta-amyloid peptide in vivo: evidence for augmentation of a 42-specific gamma secretase. Hum Mol Genet 2004; 13: 159–70.

Jessberger S, Kempermann G. Adult-born hippocampal neurons mature into activity-dependent responsiveness. Eur J Neurosci 2003; 18: 2707–12.

Jin K, Peel AL, Mao XO, Xie L, Cottrell BA, Henshall DC, et al. Increased hippocampal neurogenesis in Alzheimer's disease. Proc Natl Acad Sci USA 2004; 101: 343–7.

Kannangara TS, Eadie BD, Bostrom C, Morch K, Brocardo PS, Christie BR. GluN2A-/-Mice lack bidirectional synaptic plasticity in the dentate gyrus and perform poorly on spatial pattern separation tasks. Cereb Cortex 2014; 1500: 1–12.

Kee N, Teixeira CM, Wang AH, Frankland PW. Preferential incorporation of adult-generated granule cells into spatial memory networks in the dentate gyrus. Nat Neurosci 2007; 10: 355–62.

Kempermann G, Kuhn HG, Gage FH. Experience-induced neurogenesis in the senescent dentate gyrus. J Neurosci 1998; 18: 3206–12.

Krezymon A, Richetin K, Halley H, Roybon L, Lassalle J, Francès B, et al. Modifications of hippocampal circuits and early disruption of adult neurogenesis in the Tg2576 mouse model of Alzheimer's disease. PLoS One 2013; 8: e76497.

Kuwabara T, Hsieh J, Muotri A, Yeo G, Warashina M, Lie DC, et al. Wnt-mediated activation of Neurod1 and retro-elements during adult neurogenesis. Nat Neurosci 2009; 12: 1097–105.

Lacor PN, Buniel MC, Furlow PW, Clemente AS, Velasco PT, Wood M, et al. Abeta oligomer-induced aberrations in synapse composition shape and density provide a molecular basis for loss of connectivity in Alzheimer's disease. J Neurosci 2007; 27: 796–807.

Lazarov O, Demars MP. All in the family: how the APPs regulate neurogenesis. Front. Neurosci 2012; 6: 81.

Lesné S, Koh MT, Kotilinek L, Kayed R, Glabe CG, Yang A, et al. A specific amyloid-beta protein assembly in the brain impairs memory. Nature 2006; 440: 352–7.

Li B, Yamamori H, Tatebayashi Y, Shafit-Zagardo B, Tanimukai H, Chen S, et al. Failure of neuronal maturation in Alzheimer's disease dentate gyrus. J. Neuropathol. Exp. Neurol 2008; 67: 78–84.

Marín-Burgin A, Schinder AF. Requirement of adult-born neurons for hippocampus-dependent learning. Behav Brain Res 2012; 227: 391–9.

Marlatt MW, Bauer J, Aronica E, van Haastert ES, Hoozemans JJM, Joels M, et al. Proliferation in the Alzheimer hippocampus is due to microglia not astroglia and occurs at sites of amyloid deposition. Neural Plast 2014; 693851.

Marlatt M.W, Lucassen PJ. Neurogenesis and Alzheimer's disease: biology and pathophysiology in mice and men. Curr Alzheimer Res 2010; 7: 113–25.

Marlatt MW, Potter MC, Bayer TA, van Praag H, Lucassen PJ. Prolonged running not fluoxetine treatment increases neurogenesis but does not alter neuropathology in the 3xTg mouse model of Alzheimer's disease. Curr Topics Behav Neurosci 2013; 313–40.

Marr RA, Thomas RM, Peterson DA, Peterso DA. Insights into neurogenesis and aging: potential therapy for degenerative disease? Future Neurol 2010; 5: 527–41.

Miyata T, Maeda T, Lee JE. NeuroD is required for differentiation of the granule cells in the cerebellum and hippocampus. Genes Dev 1999; 13: 1647–52.

Mongiat L, Espósito MS, Lombardi G, Schinder AF. Reliable activation of immature neurons in the adult hippocampus. PLoS One 2009; 4: e5320.

Niibori Y, Yu TS, Epp JR, Akers KG, Josselyn SA, Frankland PW. Suppression of adult neurogenesis impairs population coding of similar contexts in hippocampal CA3 region. Nat Commun 2012; 3: 1253.

Nimchinsky EA, Sabatini BL, Svoboda K. Structure and function of dendritic spines. Annu Rev Physiol 2002; 64: 313–53.

Perry EK, Johnson M, Ekonomou A, Perry RH, Ballard C, Attems J. Neurogenic abnormalities in Alzheimer's disease differ between stages of neurogenesis and are partly related to cholinergic pathology. Neurobiol Dis 2012; 47: 155–62.

Puoliväli J, Wang J, Heikkinen T, Heikkilä M, Tapiola T, van Groen T, et al. Hippocampal A beta 42 levels correlate with spatial memory deficit in APP and PS1 double transgenic mice. Neurobiol Dis 2002; 9: 339–47.

Rodríguez JJ, Jones VC, Tabuchi M, Allan SM, Knight EM, LaFerla FM, et al. Impaired adult neurogenesis in the dentate gyrus of a triple transgenic mouse model of Alzheimer's disease. PLoS One 2008; 3: e2935.

Roybon L, Hjalt T, Stott S, Guillemot F, Li JY, Brundin P. Neurogenin2 directs granule neuroblast production and amplification while Neurod1 specifies neuronal fate during hippocampal neurogenesis. PLoS One 2009; 4: e4779.

Sahay A, Scobie KN, Hill AS, O'Carroll CM, Kheirbek MA, Burghardt NS, et al. Increasing adult hippocampal neurogenesis is sufficient to improve pattern separation. Nature 2011; 472: 466–70.

Sala C. Molecular regulation of dendritic spine shape and function. Neurosignals 2002; 11: 213–223.

Schmidt-Hieber C, Jonas P, Bischofberger J. Enhanced synaptic plasticity in newly generated granule cells of the adult hippocampus. Nature 2004; 429: 184–7.

Seib DRM, Corsini NS, Ellwanger K, Plaas C, Mateos A, Pitzer C, et al. Loss of dickkopf-1 restores neurogenesis in old age and counteracts cognitive decline. Cell Stem Cell 2013; 12: 204–14.

Shors TJ, Miesegaes G, Beylin A, Zhao M, Rydel T, Gould E. Neurogenesis in the adult is involved in the formation of trace memories. Nature 2001; 410: 372–6.

Song H, Stevens CF, Gage FH. Astroglia induce neurogenesis from adult neural stem cells. Nature 2002; 417: 39–44.

Takahashi RH, Almeida CG, Kearney PF, Yu F, Lin MT, Milner TA, et al. Oligomerization of Alzheimer's beta-amyloid within processes and synapses of cultured neurons and brain. J Neurosci 2004; 24: 3592–9.

Tashiro A, Makino H, Gage FH. Experience-specific functional modification of the dentate gyrus through adult neurogenesis: a critical period during an immature stage. J Neurosci 2007; 27: 3252–9.

Tirone F, Farioli-Vecchioli S, Micheli L, Ceccarelli M, Leonardi L. Genetic control of adult neurogenesis: interplay of differentiation proliferation and survival modulates new neurons function and memory circuits. Front Cell Neurosci 2013; 7: 59.

Toni N, Laplagne D, Zhao C, Lombardi G, Ribak CE, Gage FH, et al. Neurons born in the adult dentate gyrus form functional synapses with target cells. Nat Neurosci 2008; 11: 901–7.

Trouche S, Bontempi B, Roullet P, Rampon C. Recruitment of adult-generated neurons into functional hippocampal networks contributes to updating and strengthening of spatial memory. Proc Natl Acad Sci USA 2009; 106: 5919–24.

Van Praag H, Kempermann G, Kempermann G, Gage FH. Running increases cell proliferation and neurogenesis in the adult mouse dentate gyrus. Nat Neurosci 1999; 2: 266–70.

Verret L, Jankowsky JL, Xu GM, Borchelt DR, Rampon C. Alzheimer's-type amyloidosis in transgenic mice impairs survival of newborn neurons derived from adult hippocampal neurogenesis. J Neurosci 2007; 27: 6771–80.

Verwer RWH, Sluiter AA, Balesar RA, Baayen JC, Noske DP, Dirven CMF, et al. Mature astrocytes in the adult human neocortex express the early neuronal marker doublecortin. Brain 2007; 130: 3321–35.

Vivar C, Potter MC, Choi J, Lee JY, Stringer TP, Callaway EM, et al. Monosynaptic inputs to new neurons in the dentate gyrus. Nat Commun 2012; 3: 1107.

Wang JM, Singh C, Liu L, Irwin RW, Chen S, Chung EJ, et al. Allopregnanolone reverses neurogenic and cognitive deficits in mouse model of Alzheimer's disease. Proc Natl Acad Sci USA 2010; 107: 6498–503.

Wilcox KC, Lacor PN, Pitt J, Klein WL. Aβ oligomer-induced synapse degeneration in Alzheimer's disease. Cell Mol Neurobiol 2011; 31: 939–48.

Zhang CL, Zou Y, He W, Gage FH, Evans RM. A role for adult TLX-positive neural stem cells in learning and behaviour. Nature 2008; 451: 1004–7.

Zhao C, Teng EM, Summers RG Jr, Ming L, Gage FH. Distinct morphological stages of dentate granule neuron maturation in the adult mouse hippocampus. J Neurosci 2006; 26: 3–11.